



Published in final edited form as:

Clin Cancer Res. 2021 September 01; 27(17): 4870–4882. doi:10.1158/1078-0432.CCR-19-4191.

Activation of the interferon signaling pathway is associated with resistance to CDK4/6 inhibitors and immune checkpoint activation in ER-positive breast cancer

Carmine De Angelis^{1,2,3,4,*}, Xiaoyong Fu^{1,3,11,*}, Maria Letizia Cataldo^{1,2,3,4}, Agostina Nardone⁵, Resel Pereira^{1,2,3}, Jamunarani Veeraraghavan^{1,2,3}, Sarmistha Nanda^{1,2,3}, Lanfang Qin^{1,2,3}, Vidyalakshmi Sethunath^{1,2,3}, Tao Wang^{1,2,3}, Susan G. Hilsenbeck^{1,3}, Matteo Benelli⁶, Ilenia Migliaccio^{6,7}, Cristina Guarducci^{5,6}, Luca Malorni^{6,7}, Lacey M. Litchfield⁸, Jiangang Liu⁸, Joshua Donaldson⁹, Pier Selenica¹⁰, David N. Brown¹⁰, Britta Weigelt¹⁰, Jorge S. Reis-Filho¹⁰, Ben H. Park⁹, Sara A. Hurvitz¹¹, Dennis J. Slamon¹¹, Mothaffar F. Rimawi^{1,2,3,12}, Valerie M. Jansen⁸, Rinath Jeselsohn⁵, C. Kent Osborne^{1,2,3,12}, Rachel Schiff^{1,2,3,12}

¹Lester and Sue Smith Breast Center, Baylor College of Medicine, Houston, TX, USA

²Department of Medicine, Baylor College of Medicine, Houston, TX, USA

³Dan L Duncan Comprehensive Cancer Center, Baylor College of Medicine, Houston, TX, USA

⁴Department of Clinical Medicine and Surgery, University of Naples “Federico II”, Naples, Italy

⁵Center for Functional Cancer Epigenetics, Dana-Farber Cancer Institute, Harvard Medical School, Boston, MA, USA

⁶“Sandro Pitigliani” Translational Research Unit, Hospital of Prato, Prato, Italy,

⁷“Sandro Pitigliani” Medical Oncology Department, Hospital of Prato, Prato, Italy

⁸Eli Lilly and Company, Indianapolis, IN, USA

⁹Department of Medicine, Vanderbilt-Ingram Cancer Center, Vanderbilt University Medical Center, Nashville, TN, USA

¹⁰Department of Pathology, Memorial Sloan Kettering Cancer Center, New York, NY, USA

¹¹University of California, Los Angeles, Los Angeles, CA, USA

¹²Department of Molecular and Cellular Biology, Baylor College of Medicine, Houston, TX, USA

Abstract

Purpose: CDK4/6 inhibitors are highly effective against ER+/HER2- breast cancer (BC); however, intrinsic and acquired resistance is common. Elucidating the molecular features of sensitivity and resistance to CDK4/6i’s may lead to identification of predictive biomarkers and novel therapeutic targets, paving the way toward improving patient outcomes.

Corresponding Author: Rachel Schiff, 1 Baylor Plaza, BCM600, Houston, TX 77030; Tel: 713-798-1676; rschiff@bcm.edu.
*co-first authors

The remaining authors declare that they have no conflicts of interest.

Experimental design: Parental BC cells and their endocrine-resistant derivatives (EndoR) were used. Derivatives with acquired resistance to palbociclib (PalboR) were generated from parental and estrogen-deprivation resistant MCF7 and T47D cells. Transcriptomic and proteomic analyses were performed in palbociclib-sensitive and PalboR lines. Gene expression data from CDK4/6i neoadjuvant trials and publicly available datasets were interrogated for correlations of gene signatures and patient outcomes.

Results: Parental and EndoR BC lines showed varying degrees of sensitivity to palbociclib. Transcriptomic analysis of these cell lines identified an association between high interferon (IFN) signaling and reduced CDK4/6i sensitivity; thus an 'IFN-Related Palbociclib-Resistance Signature' (IRPS) was derived. In two neoadjuvant trials of CDK4/6i plus endocrine therapy, IRPS and other IFN-related signatures were highly enriched in patients with tumors exhibiting intrinsic resistance to CDK4/6i. PalboR derivatives displayed dramatic activation of IFN/STAT1-signaling compared to their short-term treated or untreated counterparts. In primary ER+/HER2- tumors, the IRPS score was significantly higher in lumB than lumA subtype and correlated with increased gene expression of immune checkpoints, endocrine resistance, and poor prognosis.

Conclusion: Aberrant IFN-signaling is associated with intrinsic resistance to CDK4/6i. Experimentally, acquired resistance to palbociclib is associated with activation of the IFN-pathway, warranting additional studies to clarify its involvement in resistance to CDK4/6i.

Introduction

Endocrine therapy targeting estrogen receptor (ER) activity represents the treatment backbone for patients with hormone receptor (HR) positive breast cancer (BC) of all stages. Despite the benefit of endocrine therapy, intrinsic and acquired resistance commonly occurs, negatively impacting patient outcomes. Endocrine resistance can occur through a multitude of genomic and adaptive mechanisms, and several pharmacological agents (1,2) targeting alternative or escape resistance pathways have been recently developed.

Dysregulation of cell cycle regulatory proteins, particularly those promoting progression from G1 phase to S phase, can contribute to endocrine resistance (2). In HR-positive BC, ER-dependent activation of cyclin D–cyclin-dependent kinase 4 (CDK4) and CDK6 complexes promotes passage through G1 phase by phosphorylation and inactivation of the retinoblastoma tumor-suppressor protein (Rb), which in turn releases the E2F family of transcription factors to transcribe genes required for entry into the S phase (3). The potent, selective, orally bioavailable inhibitors of CDK4 and CDK6 (CDK4/6i), palbociclib, ribociclib, and abemaciclib, in combination with an aromatase inhibitor or the selective ER degrader fulvestrant, significantly improved clinical outcomes compared with endocrine therapy alone in patients with HR-positive/HER2-negative advanced BC, and are now under clinical investigation in patients with early-stage disease (3). Despite these favorable outcomes, not all patients benefit from CDK4/6 inhibition, and the majority of patients who do initially respond ultimately progress. Deciphering the molecular features that determine sensitivity and resistance to CDK4/6 inhibition is crucial to identify predictive biomarkers and novel therapeutic targets for improving CDK4/6i efficacy and patient outcomes.

In this study, we sought to investigate the molecular profiles associated with intrinsic and acquired resistance to CDK4/6i in HR+/HER2- BC. To this end, we analyzed transcriptomic and proteomic profiles of endocrine-sensitive and -resistant BC cell lines tested for sensitivity to pharmacological or genetic inhibition of CDK4/6, studied tumor samples from patients with HR+/HER2- enrolled in neoadjuvant clinical trials evaluating CDK4/6i in combination with aromatase inhibitors, and examined preclinical models of acquired resistance to CDK4/6i. Integrating these data, we found intrinsic activation of IFN-signaling to be associated with reduced sensitivity to CDK4/6 inhibition in pre-clinical models, and with worse outcomes in patients. We also detected a remarkable up-regulation of IFN-signaling in CDK4/6i-resistant cell line derivatives. Taken together, our results suggest a role for activation of the IFN-signaling pathway in promoting both intrinsic and acquired resistance to CDK4/6 inhibitors in BC.

Materials and Methods

Cell lines, establishment of resistant lines, and reagents.

MCF7, T47D, and ZR75–1 parental (P) cells were cultured as previously described (4). The EndoR cell derivatives [resistant to long-term estrogen deprivation (EDR), to tamoxifen (TamR), and to fulvestrant (FulR)] were established as previously described (4,5). To generate resistant derivatives to palbociclib (SelleckChem), MCF7 P, MCF7 EDR, T47D P, and T47D EDR cells were exposed to progressively increasing doses of palbociclib up to 1 μ M. T47D P-LM and T47D P/PalboR-LM were cultured and developed as described previously (6). All cell lines were authenticated at the MD Anderson Characterized Cell Line Core Facility, and were tested to be mycoplasma-free by MycoAlert™ Mycoplasma Detection Kit (Lonza). Because T47D P-LM and T47D P/PalboR-LM were grown in a different media from MCF7 P, MCF7 EDR, T47D EDR and their PalboR derivatives, all parallel molecular analyses were done independently.

Cell growth assays, immunoblotting assays, qRT/PCR, and Reverse Phase Protein Arrays (RPPAs).

Detailed methods are provided in the Supplementary Methods and Suppl. Table S1 and Suppl. Table S2.

Gene expression data and analyses.

RNA-sequencing (RNA-seq) and analyses of cell models were performed as described previously (5). Gene expression data sources and data analyses are described in the Supplementary Methods.

Reverse Phase Protein Arrays (RPPAs).

RPPA analysis was performed as described previously (5). RPPA quantitative data were obtained for MCF7 P \pm palbociclib 1 μ M for 48 hours, MCF7 P/PalboR, MCF7 EDR \pm palbociclib 1 μ M for 48 hours, and MCF7 EDR/PalboR. A Benjamini–Hochberg False Discovery Rate (*FDR*) adjusted p-value (q-value) threshold of 0.05 was used to define differentially expressed proteins between groups.

Statistical analyses.

Statistical analyses were performed using R v3.5.1 and GraphPad Prism v8.01. Quantitative data are shown as mean \pm SEM from quadruplicates. Significance ($P < 0.05$) was determined by two-tailed Student's t-test, ANOVA with Dunnett/Tukey's post-hoc tests, or Pearson/Spearman correlation coefficient test.

Data availability.

All sequencing data of this study have been deposited in the National Center for Biotechnology Information Gene Expression Omnibus (GEO) database under accession codes GSE150997.

Results

Reduced sensitivity to CDK4/6 inhibition is associated with IFN-signaling in ER+ BC cell lines.

We first studied the efficacy of the CDK4/6i palbociclib in a panel of ER+ P (endocrine-sensitive) and EndoR BC cell lines (Fig 1A). The ER, PR, and HER2 mRNA and protein levels for each cell line are shown in Suppl. Fig. 1 and Suppl. Fig. 2A, respectively. The MCF7 EDR, MCF7 TamR, and T47D TamR models retained ER, but the expression of the classic ER-dependent gene PR was downregulated in MCF7 EDR and lost in MCF7 and T47D TamR compared to P cells (6). In addition, HER2 expression was increased in all of the endocrine-resistant cells compared to P cells (Suppl. Fig. 1). Palbociclib treatment resulted in a dose-dependent inhibition of cell growth of MCF7, T47D, and ZR75-1 P and EndoR cell lines, though the degree of sensitivity varied among the models. The calculated palbociclib IC₅₀ values are shown in Suppl. Fig. 2A. The MCF7 and ZR75-1 EndoR-derivatives showed higher palbociclib-sensitivity compared to their P cells, while in the T47D model only the TamR cells displayed a more pronounced growth inhibition upon palbociclib treatment compared to the counterpart P cells. Based on the distribution of the IC₅₀ values and their corresponding 95% confidence intervals (CIs), we used the cut-off value of 200 nM to define cell lines with “*high sensitivity*” (ZR75-1 TamR, ZR75-1 FulR, MCF7 TamR, T47D TamR, MCF7 EDR, ZR75-1 EDR, and MCF7 FulR) and “*low sensitivity*” (T47D P, T47D FulR, T47D EDR, MCF7 P, ZR75-1 P) to palbociclib treatment *in vitro* (Fig. 1B).

We next studied the genome-wide transcriptomic profiles of our panel of BC cell lines to identify gene expression features associated with response to CDK4/6 inhibition *in vitro*. Using the aforementioned cut-off, we first compared gene expression of ‘*low*’- ($n = 5$) vs. ‘*high*’- ($n = 7$) sensitive cell lines and performed Gene Set Enrichment Analysis (GSEA) using the hallmark gene set collection from the Molecular Signatures Database (MSigDb) (Fig. 1C). GSEA identified 6 pathways positively enriched in the “*low-sensitivity*” lines ($FDR < 0.05$), which were related to the ER-signaling (‘estrogen response early’ and ‘estrogen response late’), the immune/inflammatory response (‘interferon gamma response’, ‘interferon alpha response’, and ‘TNFA signaling via NF-kB’), and cell cycle (‘E2F targets’). We further refined this analysis by focusing on the three most sensitive cell lines (IC₅₀ < 100nM) and the three cell lines with the lowest sensitivity (IC₅₀ > 350nM)

(Suppl. Fig. 2A). The top ranked hallmark GSEA signatures enriched in the cells with low sensitivity compared to the highly sensitive cells were ‘interferon gamma response’ and ‘interferon alpha response’ (Suppl. Fig. 2B). The ‘IL6 JAK STAT3 signal’ and the ‘DNA repair’ gene sets were also enriched in our “*low sensitive*” cell models (Suppl. Fig. 2B), which is in line with a recent study showing induction of the IL-6/STAT3 pathway and a concomitant downregulation of the DNA-repair pathways in palbociclib-resistant MCF7 and T47D cell lines (7). We also observed a significant association between high IFN-signaling and less response to pharmacological (8) or genetic (9) CDK4/6 inhibition in two additional sets of ER+/HER2- cell lines (Suppl. Fig. 2C-F). Taken together, these data suggest that reduced sensitivity to CDK4/6 inhibition *in vitro* is associated with BC cell-intrinsic IFN-signaling.

To identify the IFN-stimulated genes associated with response to palbociclib, we next evaluated the correlation between the palbociclib IC50 values and expression levels of the genes that constitute the ‘interferon gamma response’ and ‘interferon alpha response’ hallmark gene sets ($n = 224$) in our cell line panel. Only genes with a mean RPKM value greater than 1 for at least one cell line were included in our analysis ($n = 171$). A total of 36 genes significantly correlated with palbociclib IC50 values ($P < 0.05$). Of those genes, 35 showed a positive (Spearman correlation > 0.5) and 1 an inverse correlation (Spearman correlation < -0.66) with palbociclib IC50 values (Fig. 1D). We termed the subset of the 35 IFN-stimulated genes whose expression was associated with reduced response to palbociclib as the ‘Interferon-Related Palbociclib-resistance Signature (IRPS)’.

Emerging data indicate that aberrant activation of the IFN/STAT1 pathway mediates drug resistance in preclinical models and is associated with poor prognosis in BC patients treated with adjuvant chemotherapy and/or radiation therapy (10,11). A gene signature for radiation and chemotherapy resistance, mainly comprising the IFN-stimulated genes ($n = 49$) [IFN-related DNA damage resistance signature (IRDS)], was previously established in preclinical models. Recently, the expression of a subset of IFN-stimulated genes (ISGs) ($n = 25$) was also found to be associated with acquired resistance to tamoxifen and radiotherapy (11). Of note, the IRPS we identified in our BC models, the IRDS, and the ISGs associated with tamoxifen- and radiotherapy-resistance showed only a partial overlap (*IFI44L*, *IFIT1*, *MX1*, *IFI44*, *IFIT3*, *LGALS3BP*, *IFI27*) (Suppl. Fig. 2G).

Enrichment for IFN-related signatures is associated with response to neoadjuvant CDK4/6 inhibitors in patients with ER+ early stage BC.

To extend our pre-clinical findings to primary human BC, we next interrogated the publicly available genome-wide expression data from the NeoPalAna trial, in which patients with treatment-naïve stage II-III HR+/HER2- BC received neoadjuvant treatment with palbociclib and anastrozole (12). In this trial, resistance was defined as Ki67 $> 2.7\%$ after 15 days of treatment (C1D15) (Fig. 2A). When we compared the transcriptomic profiles of biopsies from resistant vs. sensitive patients taken before initiation of treatment (C0D1) (Fig. 2A), the ‘interferon alpha response’ and ‘interferon gamma response’ gene sets were among the top five ranked hallmark GSEA signatures ($FDR < 0.05$) (Fig. 2B, Suppl. Table S3).

We further validated our clinical findings using baseline gene expression data from the neoMONARCH trial (13), a neoadjuvant trial evaluating the activity of the CDK4/6 inhibitor abemaciclib in combination with anastrozole in patients with early-stage HR+/HER2-BC (Fig. 2C). The ‘interferon alpha’ and ‘interferon gamma response’ were the top 2 significantly enriched gene signatures ($FDR < 0.05$) in the intrinsically resistant tumors, defined as tumors with Ki67 expression $\geq 7.4\%$ at 2 weeks and end of treatment regardless of 2-week lead in as previously described (13), compared to sensitive tumors (Ki67 2.7% at 2 weeks and end of treatment) (Fig. 2D). Notably, the IRPS gene signature was also significantly upregulated in patients intrinsically resistant to CDK4/6i in both the NeoPalAna and the neoMONARCH trials (Figs. 2B and 2D/2E).

We next examined the transcriptomic profiles of post-treatment biopsies from the neoMONARCH trial to determine the effect of neoadjuvant endocrine therapy plus abemaciclib on the IFN/IRPS signaling in sensitive and resistant patients. We found that the IFN gamma response, IFN alpha response, and our IRPS were highly enriched in the abemaciclib-resistant (n=4) vs. -sensitive (n=6) tumors after 16 weeks of treatment (Fig. 2E). Additionally, we estimated IFN signaling changes from baseline to end of therapy in sensitive vs. resistant patients. Interestingly, we observed that neoadjuvant abemaciclib treatment was associated with a decrease of IFN-signaling in the resistant tumors but an increase of IFN signaling in sensitive patients (Fig. 2E). Overall, these results suggest that intrinsic activation of IFN-signaling might predict resistance to CDK4/6i plus endocrine therapy in the clinical setting.

IFN-signaling is markedly up-regulated in cells with acquired resistance to palbociclib.

To investigate whether enhanced IFN-signaling is involved in the development of resistance to CDK4/6i, we developed MCF7 P, MCF7 EDR and T47D EDR cell line derivatives with acquired resistance to palbociclib (PalboR) and used the already established T47D P/PalboR-LM cell line (Suppl. Table S4). We studied the transcriptomes of the MCF7 P/PalboR, MCF7 EDR/PalboR, T47D P/PalboR, and T47D EDR/PalboR cell lines to identify the transcriptional alterations underlying CDK4/6i resistance. We first investigated mRNA expression levels of key G1/S cell cycle regulators, since acquired resistance to CDK4/6i frequently results from deregulation of these proteins (14). We found that multiple signal components of the cyclin D–CDK4/6–Rb axis are commonly altered in our PalboR models, including significantly elevated expression of *CCND1*, *CCND3*, *CCNE1*, *CCNE2*, *CDK2*, *CDK4*, and *CDK6*, or reduced expression of *RB1* (Suppl. Fig. 3). *RB1* mRNA expression was abolished in T47D P/PalboR-LM line as consequence of a genomic loss of *RB1* described previously in this cell line (6). To validate the changes of the cell cycle-related proteins in acquired resistance, we performed Western blot analysis for selected markers in PalboR and palbociclib-untreated cell lines. While some changes in protein expression were common across different cell lines, others were model-specific. Compared to untreated cells, the cell cycle inhibitor p27 showed reduced expression in all PalboR cells (Fig. 3). Rb expression was downregulated in MCF7 P/PalboR cell line compared with MCF7 P palbociclib-untreated counterparts, with MCF7 EDR/PalboR and T47D P/PalboR-LM cells showing virtually complete loss of expression (Fig. 3). Additionally, acquired resistance to palbociclib was associated with enhanced protein expression of CDK6 in MCF7 EDR/

PalboR and increased levels of Cyclin E1 in all PalboR cells as recently reported in several PalboR derivatives (14,15) (Fig. 3). Overall, these data suggest that the cyclin D–CDK4/6–Rb axis is altered in our PalboR models, which can probably compensate for the CDK4/6 inhibition.

We next examined the globally differentially expressed genes between PalboR models compared to their parental counterparts. Overall, 38 genes were commonly upregulated (\log_2 fold-change > 0.5, $FDR < 0.05$) in PalboR cell lines including *CCNE1* which is linked to the G1/S transition and other genes that are linked to IFN-stimulation (*i.e.* *IFI27*, *IFI44*, *an ILAR*) (Fig. 4A). Functional annotation of the overlapping upregulated genes suggested the activation of Gene Ontology processes associated with immune response and metabolic-related signatures (Suppl. Table S5). GSEA further showed that PalboR models were significantly enriched for the ‘interferon alpha response’ and ‘interferon gamma response’ hallmark gene sets (Fig. 4B, Suppl. Table S6). Our IRPS signature was also increased in all PalboR models and was significantly enriched in MCF7 EDR/PalboR (NES = 2.74) and T47D P/PalboR-LM (NES = 3.0) cell lines (Fig. 4B). Using quantitative RT-PCR, we confirmed that mRNA levels of selected key IFN-stimulated genes (*STAT1*, *IFI27*, *IFIT1*) were upregulated in PalboR cell lines compared to untreated parental counterparts (Fig. 4C). Since it was recently shown that pharmacological inhibition of CDK4/6 stimulates IFN-signaling (16), we also assessed the gene expression levels of *STAT1*, *IFI27*, and *IFIT1* in P and EDR MCF7, T47D P-LM, and T47D EDR cell lines treated with palbociclib at 1 μ M for 48 hours. Consistent with previous studies, we observed that short-term treatment with palbociclib significantly increased expression of these genes in almost all of our cell lines (Fig. 4C). Notably, however, mRNA levels of *STAT1*, *IFI27*, and *IFIT1* in all of our PalboR models were substantially higher than those detected in palbociclib-treated cells, suggesting that a further upregulation of the IFN-signaling pathway occurs at the time of acquired resistance (Fig. 4C). In keeping with the qRT-PCR results, protein expression of STAT1, a key downstream marker of Type I and II IFN-signaling, was also induced by short-term palbociclib treatment and was further enhanced at the onset of acquired resistance to the drug (Fig. 4D). Of note, exposure of cells displaying different levels of intrinsic IFN signaling and sensitivity to palbociclib (MCF7 P, T47D P-LM, and MCF7 EDR) (Fig. 2) to 3 days of exogenous IFN-gamma resulted in increased levels of p- and t-STAT1 in all cells (Suppl. Fig. 4A). Interestingly, this IFN-gamma exposure also led to a trend or significant, though small, decrease in sensitivity to palbociclib in these cell models (Suppl. Fig. 4B).

We next quantitatively measured dynamic changes in total and phosphorylated (p-) protein levels focusing on the MCF7 P and EDR cell models after short-term (48 hours) 1 μ M palbociclib treatment and with the acquisition of palbociclib-resistance, using RPPA. By comparing the proteomic profiles of our untreated MCF7 P and MCF7 EDR cell lines vs. their palbociclib-resistant derivatives, we identified 43 and 47 upregulated proteins in MCF7 P/PalboR and MCF7 EDR/PalboR, respectively (Suppl. Fig. 5, Suppl. Table S7). Notably, STAT1 was among the top consistently up-regulated proteins (Fold-change > 2) and its expression consistently increased upon short-term treatment with palbociclib and at the time of palbociclib resistance. In addition, although p-Rb remained inhibited in PalboR models, most of the E2F-regulated gene products such as Aurora kinase A, Ki67, and RRM2

returned to expression levels similar to those observed in untreated cells, suggesting an Rb-independent E2F activity in resistant lines (Suppl. Fig. 5C).

Since it has been reported that dysregulation of G1/S control, through Rb-loss or altered levels of cell cycle regulators such as Cyclin E1, may induce genomic instability and DNA damage (17,18), which may in turn favor the production of type I interferon, members of the IFIT family, and other chemokines (19), we next sought to investigate the interaction between an altered cyclin D–CDK4/6–Rb axis and IFN-signaling. Interestingly, we found that the RBsig, a gene expression signature of Rb-loss-of-function (20), was significantly enriched in the CDK4/6i intrinsically resistant tumors of the NeoPalAna and neoMONARCH trials (Suppl. Figs. 6A and 6B). Also, a modest correlation between the RBsig and IRPS signatures was found in ER+/HER2- BC from the METABRIC and TGCA datasets (Suppl. Figs. 6C and 6D). Of note, however, using MCF7 and T47D cells in which Rb was silenced by CRISPR/Cas9 to assess the correlation between Rb expression and IFN-signaling, we found no differences in total and p-STAT1 protein levels in RB knock-out compared to Rb wild-type MCF7 and T47D parental cells (Suppl. Fig. 6E). Recently, it has been suggested that CDK4/6i's increase tumor cell IFN-signaling by reducing the expression of the E2F target DNA methyl transferase 1 (*DNMT1*) (16), resulting in DNA hypomethylation at endogenous retroviral sequences and provoking a double-stranded RNA response, type III IFN production, and ultimately the expression of ISG (16). While we did see a decrease in *DNMT1* mRNA levels in the MCF7 P/PalboR and T47D EDR/PalboR compared to their palbo-sensitive counterparts MCF7 and T47D EDR (Suppl. Fig. 7), we did not find a significant correlation between baseline *DNMT1* gene expression and IFN-signaling in our P and endocrine-resistant BC cell lines ($R^2 = -0.11$, $P = 0.716$). Finally, we did not observe an enrichment for IFN-related signatures in ER+ BC harboring mutations of the DNA damage response genes, some of which has been suggested to be associated with increased sensitivity to palbociclib (21) (Suppl. Figs. 8A and 8B). Taken together, our data do not support the existence of a direct correlation between alteration of Rb signaling, especially due to Rb loss, and activation of IFN-signaling.

Since previous preclinical studies have shown that levels of ER and ER signaling are frequently altered in BC models with acquired resistance to CDK4/6 inhibitors (22,23), we also examined the expression of ER α , and ER-gene signatures in our palbociclib-resistant derivatives compared to their parental cells. Indeed, we observed a reduction in ER protein levels in MCF7 P, MCF7 EDR, and T47D P-LM cells upon acquired resistance to palbociclib (Suppl. Fig. 9A). As we previously reported, our T47D EDR cells lost ER expression and ER-dependency (4). Interestingly, however, MCF7 P/PalboR and MCF7 EDR/PalboR cells showed a significant activation of the ER signaling compared to their palbociclib-sensitive counterparts (Suppl. Fig. 9B). On the contrary, no significant enrichment of estrogen response gene sets was observed in the T47D P/PalboR-LM compared to P cells (Suppl. Fig. 9B), suggesting a different regulation of the levels of ER and ER-signaling at the time of palbociclib resistance across BC models.

IRPS predicts poor prognosis in luminal BC patients.

Since we observed an association between high IFN/STAT1 signaling and intrinsic resistance to CDK4/6i in preclinical and clinical settings, we next investigated the expression of the IRPS gene signature within primary BC profiled in TCGA and METABRIC. Within the ER+/HER2- tumors, the IRPS scores were significantly higher in luminal B vs. luminal A subtype tumors in both datasets (Fig. 5A). We next assessed whether IRPS was associated with outcome using the METABRIC dataset. Kaplan-Maier and Cox proportional hazards regression, adjusted for luminal subtype, revealed that patients with IRPS-high luminal tumors had significantly shorter breast cancer-specific-survival (BCSS) compared to patients with IRPS-low tumors (Figs. 5B and 5C). Since we found that primary BCs intrinsically resistant to CDK4/6i were also enriched for the RBSig, we further investigated the long-term outcome of ER+/HER2- luminal BC patients by taking into account the tumor expression levels of both IRPS and RBSig. We found that IRPS independently from RBSig score predicts poor BCSS in luminal BC patients regardless of luminal subtype, so that the relative impact of IRPS on BCSS is the same in RBSig+ and RBSig- patient subgroups (Figs. 5D and 5E). We further performed GSEA to identify signaling pathways associated with the RBSig and the IRPS as well as pathways selectively associated with either of these signatures (Suppl. Fig. 10). Interestingly, the hallmark “KRAS signaling up” gene set, including genes up-regulated by *KRAS* activation, was exclusively enriched in the IRPS+ BC patients (Suppl. Fig. 10). The association with outcome of selected genes from the IRPS (*IFI27*, *IFI44*, *STAT1*) was also assessed using the KMplot online tool (24). We found that high expression of *IFI27*, *IFI44*, or *STAT1* was associated with shorter relapse-free survival in ER+ BC patients treated with endocrine therapy but without chemotherapy ($n = 1,242$) (Suppl. Fig. 11).

IRPS is associated with expression of immune checkpoints and an immunosuppressive tumor microenvironment in ER+/HER2- BC patients.

We next sought to investigate the IFN-associated biological processes that may contribute to disease progression and poor clinical outcome in ER+/HER2- BC patients. Type I and II IFN-signaling generally exerts tumor-suppressive functions by promoting anti-tumor immune response, suppression of cell proliferation, and induction of apoptosis. However, under conditions of prolonged/chronic IFN-signaling, recent evidence indicates that expression of subsets of IFN-stimulated genes leads to drug resistance and favors tumor immune evasion. For example, the IFN-gamma signaling pathway induces expression of immune checkpoints such as PD-L1, PD-L2, and cytotoxic T-lymphocyte antigen-4 (*CTLA*) on tumor and stromal cell surfaces. Under persistent exposure to type I IFNs, T cells express multiple inhibitory receptors including PD-1, T-cell immunoglobulin and mucin-domain containing-3 (*TIM-3*), lymphocyte-activation gene 3 (*LAG3*), and others that are responsible for deterioration of T cell functions (“T cell exhaustion”). Since stromal and immune cells are thought to represent the primary sources of IFN in many tumor tissues, we first analyzed the correlation between IRPS scores and altered stromal and immune infiltration as defined by the ESTIMATE method in TCGA ER+/HER2- tumors (25) (Fig. 6A). ESTIMATE (Estimation of STromal and Immune cells in MAlignant Tumor tissues using Expression data) is an algorithm using transcriptional profiles of cancer tissues to impute scores inferring tumor cellularity as well as the infiltration of stromal and immune

cells based on specific gene expression signatures of stromal and immune cells. We found that the IRPS scores were not correlated with the immune scores ($R^2 = 0.008$, $P = 0.054$) or with the stromal scores ($R^2 = 0.001$, $P = 0.495$) (Fig. 6B). We next refined our analysis by estimating infiltration of specific immune cells producing either type II IFN (by activated T cells and NK cells) or type I IFN (by plasmacytoid dendritic cells, pDCs), using the CYT and pDC gene signature scores as markers for T/NK cells and pDC cells, respectively (26). As expected, IRPS-low tumors had low CYT and pDC scores (Fig. 6C, left panel). Enrichment for higher CYT or pDC scores in IRPS-medium and -high tumors suggests that these immune cells do correlate with IRPS expression in some primary ER+/HER2- tumors (Fig. 6C, **middle and right panel**). However, we also observed about 30% of high-IRPS tumors (51 out of 169) with low levels of both CYT and pDC signatures (Fig. 6C, **right panel**), suggesting cancer cell-autonomous contribution of IFN-signaling in a substantial number of primary ER+/HER2- breast tumors.

Finally, we evaluated the correlation between IRPS and mRNA levels of immune checkpoints (PD-1, PD-L1, CTLA4) in ER+/HER2- tumors. This analysis revealed a significant correlation between IRPS and expression of immune checkpoints in both the TCGA and METABRIC datasets (Figs. 6D and 6E). Notably, we also noticed that RBsig status did not affect the expression levels of immune checkpoints (Fig. 6F). To better assess IRPS status in the context of varied immune cell compositions in breast tumors, we inferred the abundance of immune cell subpopulations in ER+/HER2- tumors using the CIBERSORT analytical tool (27). Interestingly, among the immune subtypes positively correlated with the IRPS scores, the top two were the M1-polarized immunostimulatory macrophages, which are activated by IFN-gamma (28), and the forkhead box P3 (FOXP3+)-CD4+ T lymphocytes (TReg), which suppress T cell functions and promote T cell exhaustion (Fig. 6G) (29). Overall, these results suggest that intrinsic activation of IFN-signaling in primary ER+/HER2- BC is associated with an immunosuppressive index, which may contribute to immune escape and overall poor prognosis.

Discussion

Herein, we report aberrant activation of IFN-signaling as a potential biomarker linked to resistance to CDK4/6i in both ER+/HER2- BC cell lines and patient tumors from two neoadjuvant clinical trials. Further, we found hyperactive IFN-signaling in ER+/HER2- BC preclinical models with acquired resistance to palbociclib, suggesting its potential involvement in resistance.

Type I or type II IFN-mediated signaling plays a critical role in the human immune response (30). The binding of IFNs to their receptors activates Janus-activated kinases (Jak1, Jak2, and Tyk2), which in turn phosphorylate and activate STAT1. Activated STAT1 forms homodimers [known as gamma-IFN activation factor (GAF)] or heterodimers with STAT2 and IRF9 [known as IFN-stimulated transcription factor gamma 3 (ISGF3)] that are translocated to the nucleus favoring the transcription of IFN stimulated genes (ISG) by binding to the gamma-IFN-activated sequence (GAS) or IFN-stimulated response elements (ISRE), respectively. The expression of ISG is classically associated with pro-inflammatory, pro-apoptotic, and tumor-suppressive functions (30). However, several studies have shown

that constitutive activation of the IFN-signaling pathway promotes tumor growth, metastasis, and resistance to chemotherapy and radiation (31–36). Interestingly, it has been shown that expression levels of ISG are increased in BC cell lines with acquired resistance to estrogen deprivation (37) and to tamoxifen (11). High baseline expression of ISGs has been associated with reduced response to neoadjuvant AI treatment in postmenopausal BC patients (38) and worse outcome after tamoxifen treatment (11). Notably, targeting ISG resulted in a sensitization of chemotherapy (31,39) and hormonal therapy (37) resistant cells, suggesting their role in determining resistance to these drugs. Our data indicate IFN-signaling as an important pathway associated with both intrinsic and acquired resistance to CDK4/6i. We have demonstrated that baseline high IFN-signaling is associated with reduced sensitivity to the CDK4/6i palbociclib *in vitro*, and with intrinsic resistance to palbociclib or abemaciclib in combination with aromatase inhibitor in BC patients. We also showed that the IFN pathway is consistently dysregulated in 2 sets of palbociclib-resistant BC cells.

In BC preclinical models, CDK4/6i's have been shown to synergize with immunotherapy (40). CDK4/6i's enhanced tumor immunogenicity by stimulating IFN-signaling, tumor antigen presentation, and cytotoxic T-cell functions, and by suppressing the proliferation of regulatory T cells (Treg) (40). These intriguing data provided the rationale for ongoing clinical trials testing CDK4/6i in combination with immune-checkpoint inhibitors ([NCT02778685](#); [NCT02779751](#); [NCT03147287](#)). However, IFN-signaling regulates PD-1 ligand expression on stromal and tumor cells (41), and up-regulation of PD-L1, while associated with increased sensitivity to immune checkpoint inhibitors, has also been associated with intrinsic and acquired resistance to immunotherapy (42). In addition, it has been demonstrated that sustained IFN-signaling leads to adaptive resistance to immune checkpoint therapy through a PD-L1-independent multigenic program in melanoma (43). Specifically, prolonged IFN-gamma signaling favors STAT1-dependent expression of interferon-stimulated genes and ligands for multiple T cell inhibitory receptors on resistant tumor cells which promote T cell exhaustion (43). Our data raise the question of whether intermittent rather than concomitant administration of CDK4/6i's with immune checkpoint inhibitors would represent a more effective therapeutic scheme for patients with ER+/HER2- BC. We speculate that prolonged interferon signaling due to CDK4/6 blockade may jeopardize the antitumor activity of at least some immune checkpoint blockade strategies.

In the present study, we have derived an IFN-related gene signature associated with resistance to palbociclib (IRPS), using a panel of clinically relevant BC cell lines. In two neoadjuvant trials of endocrine therapy plus CDK4/6i, tumors with high IRPS were less likely respond to treatment as defined by reduction of the proliferation antigen Ki67. Higher Ki67 expression after neoadjuvant endocrine therapy has been associated with a lower recurrence-free survival rate (44,45). Our analysis of the publicly available datasets revealed that IRPS signaling was higher in the less endocrine-sensitive and more aggressive luminal B subtype compared to the luminal A subtype, and that high expression of the IRPS signature was associated with worse BCSS survival. Importantly, high expression of key IFN-stimulated genes of the IRPS signature predict reduced response to adjuvant endocrine therapy. Our observations suggest that tumor profiling before starting therapy could be relevant for identifying patients with high IFN-signaling who will not benefit from endocrine therapy alone or in combination with CDK4/6 blockade. This hypothesis

may be tested in currently ongoing clinical trials investigating adjuvant endocrine therapy ± CDK4/6i ([NCT02513394](#), [NCT01864746](#), [NCT03078751](#), [NCT03155997](#)). If validated, evaluation of IFN-signaling during the course of treatment might be helpful to monitor metastatic disease, as our data show that IFN-signaling is induced by treatment *in vitro*, and cell lines with acquired resistance to CDK4/6i commonly display a hyperactive IFN-signaling, irrespective of their basal level.

Similar to a previous study (26), our results also indicate that while in some ER+/HER2- primary breast tumors immune cell infiltration correlates with the IRPS signature, in others IRPS activation is independent of the presence of IFN-producing immune cells. This suggests a cancer cell-autonomous IFN-signaling, which corroborates our *in vitro* data from tumor cell cultures in the absence of immune cells. Tumor immune infiltration varies and has different impact on outcomes across BC subtypes. Overall, luminal breast tumors are characterized by low levels of stromal and intratumoral tumor-infiltrating lymphocytes, and their levels are not associated with prognosis (46). An earlier study showed that BCs with increased STAT1 mRNA levels exhibited elevated expression of genes associated with macrophages and immunosuppressive T lymphocytes, and a worse outcome (47). Similarly, we found that IRPS correlates with M1 polarized macrophages and regulatory T cells infiltration, and immune checkpoints expression. M1 macrophage phenotype is classically associated with inflammation and antitumor functions. However, emerging data indicate that inappropriate or prolonged macrophage activation can result in immune dysregulation and tumor progression (48). We speculate that chronic IFN-signaling may promote an immune-suppressive microenvironment by favoring the expression of immune checkpoints and TRegs infiltration and by altering classical functions of M1 macrophages that can partly explain worse long-term outcomes in patients with high IRPS. However, we recognize that interaction between IFN-signaling by tumor cells and tumor immune microenvironment should be further investigated.

In this study, we were not able to clarify the molecular basis for hyperactive IFN-signaling in treatment-naïve BC and at the onset of CDK4/6i resistance. De-regulated Rb- and DNA damage response pathways have been suggested as potential inducers of IFN-signaling, but our data do not support an interplay between these pathways. While, by exposing ER+ BC cells to short-term exogenous IFN-gamma, we demonstrated that acute activation of IFN-signaling slightly reduced *in vitro* sensitivity to palbociclib, additional future studies will be needed to further establish the role and the mechanisms of hyperactive IFN-signaling in mediating CDK4/6i resistance.

In conclusion, we show here that activation of the IFN-signaling pathway is associated with intrinsic and acquired resistance to CDK4/6i in BC. Future studies are needed to uncover mechanistic insights on activation of IFN-signaling in tumor cells and how it is involved in resistance to CDK4/6i, and also to validate the predictive and/or prognostic value of IFN-signaling and our IRPS signature in ER+/HER2- BC. These efforts may also allow identification of the key candidate genes that will be tested as novel therapeutic targets to prevent/reverse resistance to CDK4/6i.

Supplementary Material

Refer to Web version on PubMed Central for supplementary material.

Acknowledgments:

We thank Fuli Jia, Myra Costello, and Dr. Kimberley Holloway for performing the RPPA assays. This work was supported in part by the Cancer Prevention & Research Institute of Texas CPRIT RP140102 and the Conquer Cancer Foundation—Gianni Bonadonna Breast Cancer Research Fellowship (CDA), the Breast Cancer Research Foundation 16–142, 17–143, 18–145, 19–145, 20–145 (RS, CKO, BW, JSR-F), National Institutes of Health (NIH) Breast Cancer Specialized Programs of Research Excellence Grant P50CA186784 (CKO and RS), and NIH/NCI Cancer Center Support Grant P30CA125123 (CKO, RS, XF, TW, SGH, MFR, JV) and P30CA008748 (MSK; PS, DNB, BW, JSR-F). This work was also supported by the Proteomics & Metabolomics Core at Baylor College of Medicine (BCM) with funding from CPRIT RP120092 (Shixia Huang and Dean Edwards).

Disclosure of Potential Conflicts of Interest: **CKO** is a consultant/advisory board/member of data monitoring committee for AstraZeneca, GlaxoSmithKline, Pfizer, Tolmar Therapeutics, Genentech, and Lilly. **RS** is a paid consultant for MacroGenics and reports receiving commercial research grants from AstraZeneca, GlaxoSmithKline, Gilead Sciences, and PUMA Biotechnology. **LML** and **JL** are employees and shareholders of Eli Lilly and Company. **RJ** is a consultant/advisory board member for Pfizer. **JSR-F** has received personal/consultancy fees from VolitionRx, Paige.AI, Goldman Sachs, REPARE Therapeutics, GRAIL, Ventana Medical Systems, Roche, Genentech, and InVivo outside of the scope of the submitted work. **MFR** has received research support from GlaxoSmithKline (to institution), and consults with Genentech, Novartis, Daiichi, and MacroGenics. **VMJ** is a previous employee and current stockholder of Lilly. **SAH** has received research support (to institution) from Ambrx, Amgen, Bayer, Daiichi-Sankyo, Genentech/Roche, GSK, Immunomedics, and Lilly. **BHP** is a paid consultant for Loxo Oncology and had prior ownership interest and is a paid consultant for Jackson Laboratories. **LM** is consultant/advisory board member for Novartis and Pfizer and received research support from Novartis and Pfizer. **MB** is a paid consultant for Novartis. **DJS** is a member of the board of directors for BioMarin; is a paid consultant for Novartis, Eli Lilly, and Pfizer; has received research support from Novartis; and has ownership interests in Pfizer and Novartis.

References

1. Jeselsohn R, De Angelis C, Brown M, Schiff R. The Evolving Role of the Estrogen Receptor Mutations in Endocrine Therapy-Resistant Breast Cancer. *Curr Oncol Rep* [Internet]. 2017;19:35. Available from: <http://www.ncbi.nlm.nih.gov/pubmed/28374222> [PubMed: 28374222]
2. Nardone A, De Angelis C, Trivedi M V, Osborne CK, Schiff R. The changing role of ER in endocrine resistance. *Breast* [Internet]. 2015;24 Suppl 2:S60–6. Available from: <http://www.ncbi.nlm.nih.gov/pubmed/26271713> [PubMed: 26271713]
3. Pernas S, Tolaney SM, Winer EP, Goel S. CDK4/6 inhibition in breast cancer: current practice and future directions. *Ther Adv Med Oncol* [Internet]. 2018;10:1758835918786451. Available from: <http://www.ncbi.nlm.nih.gov/pubmed/30038670>
4. Nardone A, Weir H, Delpuech O, Brown H, De Angelis C, Cataldo ML, et al. The oral selective oestrogen receptor degrader (SERD) AZD9496 is comparable to fulvestrant in antagonising ER and circumventing endocrine resistance. *Br J Cancer* [Internet]. 2019;120:331–9. Available from: <http://www.ncbi.nlm.nih.gov/pubmed/30555156> [PubMed: 30555156]
5. Fu X, Jeselsohn R, Pereira R, Hollingsworth EF, Creighton CJ, Li F, et al. FOXA1 overexpression mediates endocrine resistance by altering the ER transcriptome and IL-8 expression in ER-positive breast cancer. *Proc Natl Acad Sci U S A* [Internet]. 2016;113:E6600–9. Available from: <http://www.ncbi.nlm.nih.gov/pubmed/27791031> [PubMed: 27791031]
6. Pink JJ, Jordan VC. Models of estrogen receptor regulation by estrogens and antiestrogens in breast cancer cell lines. *Cancer Res* [Internet]. 1996;56:2321–30. Available from: <http://www.ncbi.nlm.nih.gov/pubmed/8625307> [PubMed: 8625307]
7. Kettner NM, Vijayaraghavan S, Durak MG, Bui T, Kohansal M, Ha MJ, et al. Combined Inhibition of STAT3 and DNA Repair in Palbociclib-Resistant ER-Positive Breast Cancer. *Clin Cancer Res* [Internet]. 2019;25:3996–4013. Available from: <http://www.ncbi.nlm.nih.gov/pubmed/30867218> [PubMed: 30867218]

8. Finn RS, Dering J, Conklin D, Kalous O, Cohen DJ, Desai AJ, et al. PD 0332991, a selective cyclin D kinase 4/6 inhibitor, preferentially inhibits proliferation of luminal estrogen receptor-positive human breast cancer cell lines in vitro. *Breast Cancer Res* [Internet]. 2009;11:R77. Available from: <http://www.ncbi.nlm.nih.gov/pubmed/19874578> [PubMed: 19874578]
9. McFarland JM, Ho ZV, Kugener G, Dempster JM, Montgomery PG, Bryan JG, et al. Improved estimation of cancer dependencies from large-scale RNAi screens using model-based normalization and data integration. *Nat Commun* [Internet]. 2018;9:4610. Available from: <http://www.ncbi.nlm.nih.gov/pubmed/30389920> [PubMed: 30389920]
10. Khodarev NN, Roizman B, Weichselbaum RR. Molecular pathways: interferon/stat1 pathway: role in the tumor resistance to genotoxic stress and aggressive growth. *Clin Cancer Res* [Internet]. 2012;18:3015–21. Available from: <http://www.ncbi.nlm.nih.gov/pubmed/22615451> [PubMed: 22615451]
11. Post AEM, Smid M, Nagelkerke A, Martens JWM, Bussink J, Sweep FCGJ, et al. Interferon-Stimulated Genes Are Involved in Cross-resistance to Radiotherapy in Tamoxifen-Resistant Breast Cancer. *Clin Cancer Res* [Internet]. 2018;24:3397–408. Available from: <http://www.ncbi.nlm.nih.gov/pubmed/29661777> [PubMed: 29661777]
12. Ma CX, Gao F, Luo J, Northfelt DW, Goetz M, Forero A, et al. NeoPalAna: Neoadjuvant Palbociclib, a Cyclin-Dependent Kinase 4/6 Inhibitor, and Anastrozole for Clinical Stage 2 or 3 Estrogen Receptor-Positive Breast Cancer. *Clin Cancer Res* [Internet]. 2017;23:4055–65. Available from: <http://www.ncbi.nlm.nih.gov/pubmed/28270497> [PubMed: 28270497]
13. Hurvitz SA, Martín M, Press MF, Chan D, Fernandez-Abad M, Petru E, et al. Potent cell cycle inhibition and upregulation of immune response with abemaciclib and anastrozole in neoMONARCH, Phase 2 neoadjuvant study in HR+/HER2- breast cancer. *Clin Cancer Res* [Internet]. 2019; Available from: <http://www.ncbi.nlm.nih.gov/pubmed/31615937>
14. Portman N, Alexandrou S, Carson E, Wang S, Lim E, Caldon CE. Overcoming CDK4/6 inhibitor resistance in ER-positive breast cancer. *Endocr Relat Cancer* [Internet]. 2019;R15–30. Available from: <https://erc.bioscientifica.com/view/journals/erc/26/1/ERC-18-0317.xml> [PubMed: 30389903]
15. Guarducci C, Bonechi M, Benelli M, Biagioni C, Boccalini G, Romagnoli D, et al. Cyclin E1 and Rb modulation as common events at time of resistance to palbociclib in hormone receptor-positive breast cancer. *NPJ breast cancer* [Internet]. 2018;4:38. Available from: <http://www.ncbi.nlm.nih.gov/pubmed/30511015> [PubMed: 30511015]
16. Goel S, DeCristo MJ, Watt AC, BrinJones H, Sceneay J, Li BB, et al. CDK4/6 inhibition triggers anti-tumour immunity. *Nature* [Internet]. 2017;548:471–5. Available from: <http://www.ncbi.nlm.nih.gov/pubmed/28813415> [PubMed: 28813415]
17. van Harn T, Fojtj F, van Vugt M, Banerjee R, Yang F, Oostra A, et al. Loss of Rb proteins causes genomic instability in the absence of mitogenic signaling. *Genes Dev* [Internet]. 2010;24:1377–88. Available from: <http://www.ncbi.nlm.nih.gov/pubmed/20551164> [PubMed: 20551164]
18. Macheret M, Halazonetis TD. Intragenic origins due to short G1 phases underlie oncogene-induced DNA replication stress. *Nature* [Internet]. 2018;555:112–6. Available from: <http://www.ncbi.nlm.nih.gov/pubmed/29466339> [PubMed: 29466339]
19. Abe T, Harashima A, Xia T, Konno H, Konno K, Morales A, et al. STING recognition of cytoplasmic DNA instigates cellular defense. *Mol Cell* [Internet]. 2013;50:5–15. Available from: <http://www.ncbi.nlm.nih.gov/pubmed/23478444> [PubMed: 23478444]
20. Malorni L, Piazza S, Ciani Y, Guarducci C, Bonechi M, Biagioni C, et al. A gene expression signature of retinoblastoma loss-of-function is a predictive biomarker of resistance to palbociclib in breast cancer cell lines and is prognostic in patients with ER positive early breast cancer. *Oncotarget* [Internet]. 2016;7:68012–22. Available from: <http://www.ncbi.nlm.nih.gov/pubmed/27634906> [PubMed: 27634906]
21. Haricharan S, Punturi N, Singh P, Holloway KR, Anurag M, Schmelz J, et al. Loss of MutL Disrupts CHK2-Dependent Cell-Cycle Control through CDK4/6 to Promote Intrinsic Endocrine Therapy Resistance in Primary Breast Cancer. *Cancer Discov* [Internet]. 2017;7:1168–83. Available from: <http://www.ncbi.nlm.nih.gov/pubmed/28801307> [PubMed: 28801307]

22. Goel S, DeCristo MJ, McAllister SS, Zhao JJ. CDK4/6 Inhibition in Cancer: Beyond Cell Cycle Arrest. *Trends Cell Biol* [Internet]. 2018;28:911–25. Available from: <http://www.ncbi.nlm.nih.gov/pubmed/30061045> [PubMed: 30061045]
23. Guarducci C, Bonechi M, Boccalini G, Benelli M, Risi E, Di Leo A, et al. Mechanisms of Resistance to CDK4/6 Inhibitors in Breast Cancer and Potential Biomarkers of Response. *Breast Care (Basel)* [Internet]. 2017;12:304–8. Available from: <http://www.ncbi.nlm.nih.gov/pubmed/29234249> [PubMed: 29234249]
24. Györfy B, Lanczky A, Eklund AC, Denkert C, Budczies J, Li Q, et al. An online survival analysis tool to rapidly assess the effect of 22,277 genes on breast cancer prognosis using microarray data of 1,809 patients. *Breast Cancer Res Treat* [Internet]. 2010;123:725–31. Available from: <http://www.ncbi.nlm.nih.gov/pubmed/20020197> [PubMed: 20020197]
25. Yoshihara K, Shahmoradgoli M, Martínez E, Vegesna R, Kim H, Torres-Garcia W, et al. Inferring tumour purity and stromal and immune cell admixture from expression data. *Nat Commun* [Internet]. 2013;4:2612. Available from: <http://www.ncbi.nlm.nih.gov/pubmed/24113773> [PubMed: 24113773]
26. Liu H, Golji J, Brodeur LK, Chung FS, Chen JT, DeBeaumont RS, et al. Tumor-derived IFN triggers chronic pathway agonism and sensitivity to ADAR loss. *Nat Med* [Internet]. 2019;25:95–102. Available from: <http://www.ncbi.nlm.nih.gov/pubmed/30559422> [PubMed: 30559422]
27. Newman AM, Liu CL, Green MR, Gentles AJ, Feng W, Xu Y, et al. Robust enumeration of cell subsets from tissue expression profiles. *Nat Methods* [Internet]. 2015;12:453–7. Available from: <http://www.ncbi.nlm.nih.gov/pubmed/25822800> [PubMed: 25822800]
28. Raggi F, Pelassa S, Pierobon D, Penco F, Gattorno M, Novelli F, et al. Regulation of Human Macrophage M1-M2 Polarization Balance by Hypoxia and the Triggering Receptor Expressed on Myeloid Cells-1. *Front Immunol* [Internet]. 2017;8:1097. Available from: <http://www.ncbi.nlm.nih.gov/pubmed/28936211> [PubMed: 28936211]
29. Wherry EJ, Kurachi M. Molecular and cellular insights into T cell exhaustion. *Nat Rev Immunol* [Internet]. 2015;15:486–99. Available from: <http://www.ncbi.nlm.nih.gov/pubmed/26205583> [PubMed: 26205583]
30. Platanius LC. Mechanisms of type-I- and type-II-interferon-mediated signalling. *Nat Rev Immunol* [Internet]. 2005;5:375–86. Available from: <http://www.ncbi.nlm.nih.gov/pubmed/15864272> [PubMed: 15864272]
31. Weichselbaum RR, Ishwaran H, Yoon T, Nuyten DSA, Baker SW, Khodarev N, et al. An interferon-related gene signature for DNA damage resistance is a predictive marker for chemotherapy and radiation for breast cancer. *Proc Natl Acad Sci U S A* [Internet]. 2008;105:18490–5. Available from: <http://www.ncbi.nlm.nih.gov/pubmed/19001271> [PubMed: 19001271]
32. Rickardson L, Fryknäs M, Dhar S, Lövborg H, Gullbo J, Rydåker M, et al. Identification of molecular mechanisms for cellular drug resistance by combining drug activity and gene expression profiles. *Br J Cancer* [Internet]. 2005;93:483–92. Available from: <http://www.ncbi.nlm.nih.gov/pubmed/16012520> [PubMed: 16012520]
33. Lan Q, Peyvandi S, Duffey N, Huang Y-T, Barras D, Held W, et al. Type I interferon/IRF7 axis instigates chemotherapy-induced immunological dormancy in breast cancer. *Oncogene* [Internet]. 2019;38:2814–29. Available from: <http://www.ncbi.nlm.nih.gov/pubmed/30546090> [PubMed: 30546090]
34. Luker KE, Pica CM, Schreiber RD, Piwnica-Worms D. Overexpression of IRF9 confers resistance to antimicrotubule agents in breast cancer cells. *Cancer Res* [Internet]. 2001;61:6540–7. Available from: <http://www.ncbi.nlm.nih.gov/pubmed/11522652> [PubMed: 11522652]
35. Qadir AS, Ceppi P, Brockway S, Law C, Mu L, Khodarev NN, et al. CD95/Fas Increases Stemness in Cancer Cells by Inducing a STAT1-Dependent Type I Interferon Response. *Cell Rep* [Internet]. 2017;18:2373–86. Available from: <http://www.ncbi.nlm.nih.gov/pubmed/28273453> [PubMed: 28273453]
36. Khodarev NN, Beckett M, Labay E, Darga T, Roizman B, Weichselbaum RR. STAT1 is overexpressed in tumors selected for radioresistance and confers protection from radiation in transduced sensitive cells. *Proc Natl Acad Sci U S A* [Internet]. 2004;101:1714–9. Available from: <http://www.ncbi.nlm.nih.gov/pubmed/14755057> [PubMed: 14755057]

37. Choi HJ, Lui A, Ogony J, Jan R, Sims PJ, Lewis-Wambi J. Targeting interferon response genes sensitizes aromatase inhibitor resistant breast cancer cells to estrogen-induced cell death. *Breast Cancer Res* [Internet]. 2015;17:6. Available from: <http://www.ncbi.nlm.nih.gov/pubmed/25588716> [PubMed: 25588716]
38. Dunbier AK, Ghazoui Z, Anderson H, Salter J, Nerurkar A, Osin P, et al. Molecular profiling of aromatase inhibitor-treated postmenopausal breast tumors identifies immune-related correlates of resistance. *Clin Cancer Res* [Internet]. 2013;19:2775–86. Available from: <http://www.ncbi.nlm.nih.gov/pubmed/23493347> [PubMed: 23493347]
39. Gaston J, Cheradame L, Yvonne V, Deas O, Poupon M-F, Judde J-G, et al. Intracellular STING inactivation sensitizes breast cancer cells to genotoxic agents. *Oncotarget* [Internet]. 2016;7:77205–24. Available from: <http://www.ncbi.nlm.nih.gov/pubmed/27791205> [PubMed: 27791205]
40. Schaer DA, Beckmann RP, Dempsey JA, Huber L, Forest A, Amaladas N, et al. The CDK4/6 Inhibitor Abemaciclib Induces a T Cell Inflamed Tumor Microenvironment and Enhances the Efficacy of PD-L1 Checkpoint Blockade. *Cell Rep* [Internet]. 2018;22:2978–94. Available from: <http://www.ncbi.nlm.nih.gov/pubmed/29539425> [PubMed: 29539425]
41. Garcia-Diaz A, Shin DS, Moreno BH, Saco J, Escuin-Ordinas H, Rodriguez GA, et al. Interferon Receptor Signaling Pathways Regulating PD-L1 and PD-L2 Expression. *Cell Rep* [Internet]. 2017;19:1189–201. Available from: <http://www.ncbi.nlm.nih.gov/pubmed/28494868> [PubMed: 28494868]
42. Gide TN, Wilmott JS, Scolyer RA, Long GV. Primary and Acquired Resistance to Immune Checkpoint Inhibitors in Metastatic Melanoma. *Clin Cancer Res* [Internet]. 2018;24:1260–70. Available from: <http://www.ncbi.nlm.nih.gov/pubmed/29127120> [PubMed: 29127120]
43. Benci JL, Xu B, Qiu Y, Wu TJ, Dada H, Twyman-Saint Victor C, et al. Tumor Interferon Signaling Regulates a Multigenic Resistance Program to Immune Checkpoint Blockade. *Cell* [Internet]. 2016;167:1540–1554.e12. Available from: <http://www.ncbi.nlm.nih.gov/pubmed/27912061>
44. Ellis MJ, Suman VJ, Hoog J, Goncalves R, Sanati S, Creighton CJ, et al. Ki67 Proliferation Index as a Tool for Chemotherapy Decisions During and After Neoadjuvant Aromatase Inhibitor Treatment of Breast Cancer: Results From the American College of Surgeons Oncology Group Z1031 Trial (Alliance). *J Clin Oncol* [Internet]. 2017;35:1061–9. Available from: <http://www.ncbi.nlm.nih.gov/pubmed/28045625> [PubMed: 28045625]
45. Dowsett M, Smith IE, Ebbs SR, Dixon JM, Skene A, A'Hern R, et al. Prognostic value of Ki67 expression after short-term presurgical endocrine therapy for primary breast cancer. *J Natl Cancer Inst* [Internet]. 2007;99:167–70. Available from: <http://www.ncbi.nlm.nih.gov/pubmed/17228000> [PubMed: 17228000]
46. Solinas C, Carbognin L, De Silva P, Criscitiello C, Lambertini M. Tumor-infiltrating lymphocytes in breast cancer according to tumor subtype: Current state of the art. *Breast* [Internet]. 2017;35:142–50. Available from: <http://www.ncbi.nlm.nih.gov/pubmed/28735162> [PubMed: 28735162]
47. Tymoszyk P, Charoentong P, Hackl H, Spilka R, Müller-Holzner E, Trajanoski Z, et al. High STAT1 mRNA levels but not its tyrosine phosphorylation are associated with macrophage infiltration and bad prognosis in breast cancer. *BMC Cancer* [Internet]. 2014;14:257. Available from: <http://www.ncbi.nlm.nih.gov/pubmed/24725474> [PubMed: 24725474]
48. Poh AR, Ernst M. Targeting Macrophages in Cancer: From Bench to Bedside. *Front Oncol* [Internet]. 2018;8:49. Available from: <http://www.ncbi.nlm.nih.gov/pubmed/29594035> [PubMed: 29594035]

Translational Relevance

The combination of CDK4/6 inhibitors (i) with endocrine therapy represents the standard of care for patients with ER+/HER2- advanced breast cancer. Despite marked improvement in patient outcomes with this combination, *de novo* and acquired resistance is common. Our study reveals an inverse association between response to CDK4/6i and interferon signaling pathway activation. We demonstrate that activation of the IFN signaling pathway is associated with intrinsic and acquired resistance to CDK4/6i. Clinically, enrichment for IFN-related gene signatures is associated with resistance to neoadjuvant CDK4/6i in early stage ER+ breast cancer. Furthermore, primary ER+/HER2- breast cancers displaying *intrinsic* high interferon signaling are associated with poor prognosis. Overall, our findings suggest that the interferon pathway may offer predictive biomarkers to identify patients whose disease is less likely to respond to CDK4/6i, and potential actionable targets for the development of novel therapeutic approaches to prevent/reverse resistance to CDK4/6i.

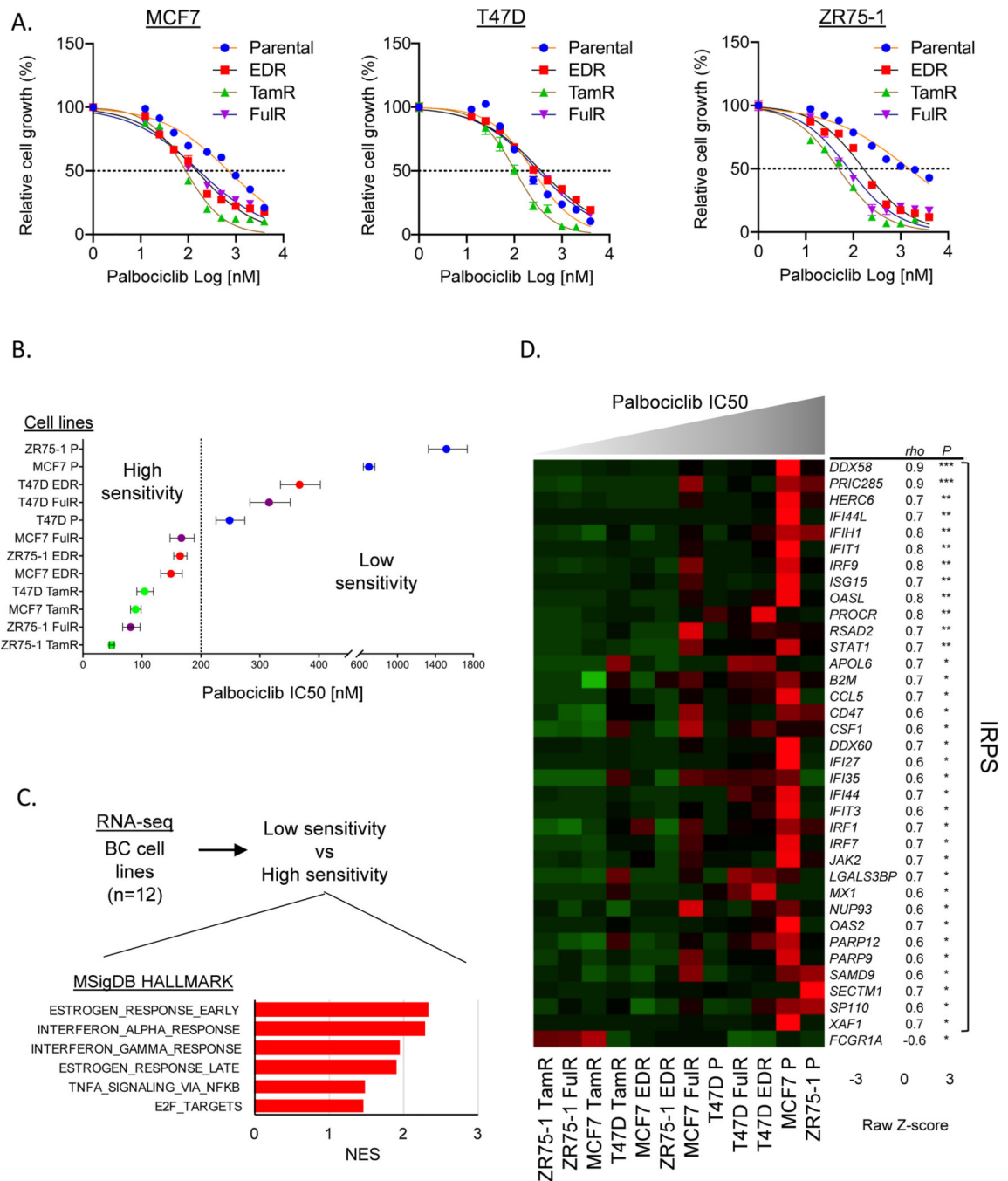


Figure 1. Reduced sensitivity to CDK4/6 inhibition is associated with IFN-signaling in ER+ BC cell lines.

A. Palbociclib responses of MCF7, T47D, and ZR75-1 parental (P) cell lines and their endocrine-resistant derivatives [EDR, estrogen deprivation-resistant; FulR, fulvestrant-resistant; TamR, tamoxifen-resistant] were measured by 6-day cell growth assays. Cells were plated in their original media. Medium was replaced the next day with regular medium or palbociclib-containing medium, and replaced again after 3 days. Data were analyzed by GraphPad Prism to generate drug response curves and relative IC50 values using the log

(inhibitor) versus response-variable slope (four parameters) model (bars, SEM). **B**, IC50s (nM) for each cell line with 95% confidence intervals; the vertical line indicates the cut-off used to define cell lines with “high” or “low” sensitivity to palbociclib. **C**, Upregulated hallmark signatures in cell lines with “low” vs. “high” sensitivity to palbociclib. Normalized enrichment scores (NES) were provided according to GSEA; for all gene sets $FDR < 0.05$. **D**, Heatmap showing genes belonging to the IFN-alpha response and/or IFN-gamma response gene signatures significantly correlated with palbociclib IC50 values in P and endocrine-resistant derivative BC cell lines. Spearman correlation coefficient test, * $P < 0.05$, ** $P < 0.01$, *** $P < 0.001$.

Author Manuscript

Author Manuscript

Author Manuscript

Author Manuscript

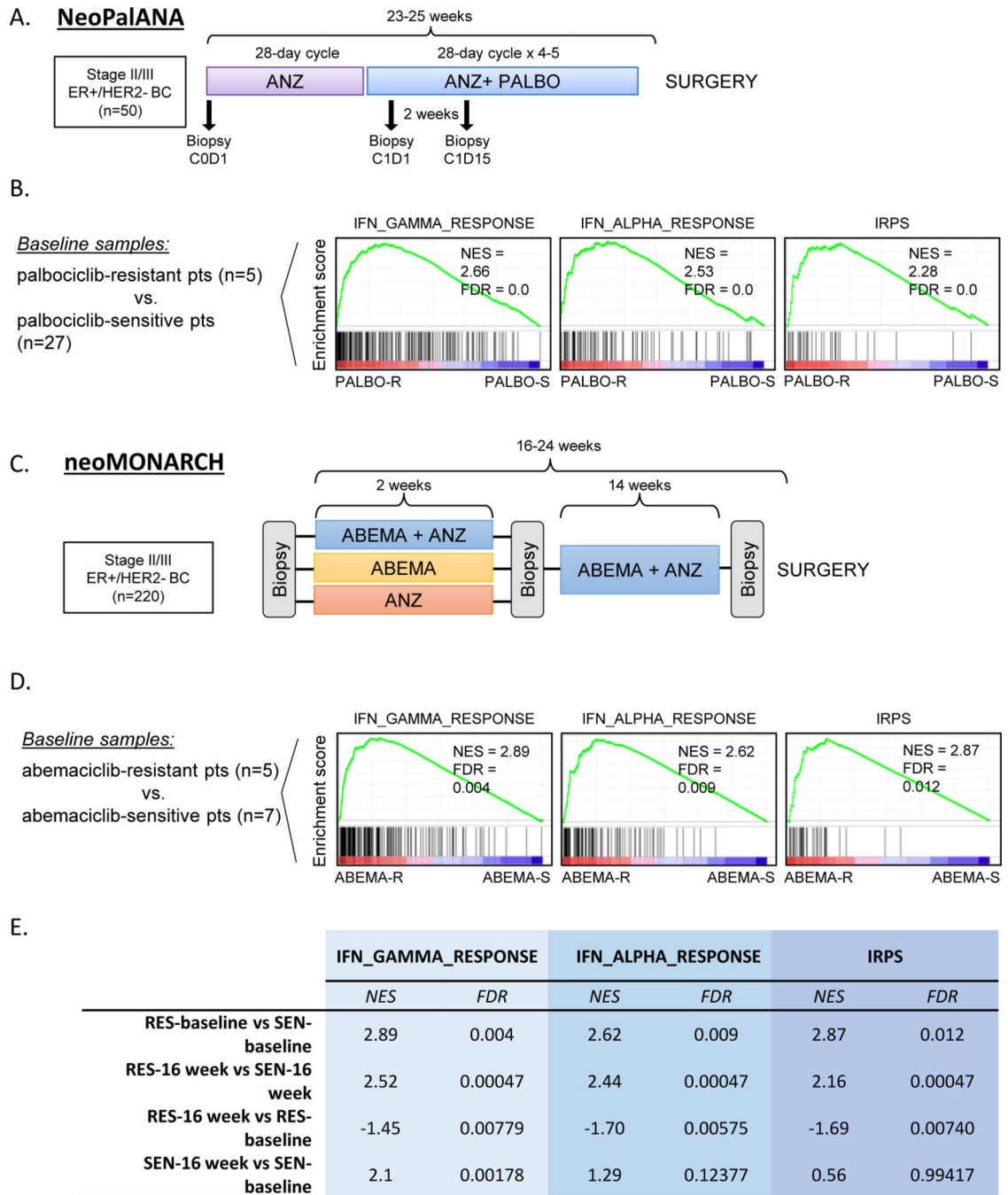


Figure 2. Enrichment for IFN-related signatures is associated with response to neoadjuvant CDK4/6 inhibitors in patients with ER+ early stage BC.

A-B, NeoPalAna study design (A) and GSEA plots of IFN-alpha response, IFN-gamma response, and IRPS signatures in baseline samples of palbociclib-resistant ($n = 5$) vs palbociclib-sensitive ($n = 27$) ER+ BC patients (B). **C-E,** neoMONARCH study design (C), GSEA plots of IFN-alpha response, IFN-gamma response, and IRPS signatures in baseline samples of abemaciclib-resistant ($n = 5$) vs abemaciclib-sensitive ($n = 7$) ER+ BC patients (D), and GSEA of IFN-alpha response, IFN-gamma response, and IRPS

signatures in baseline and post-16 weeks of treatment samples of abemaciclib-resistant vs -sensitive ER+ BC patients (E). ABEMA, abemaciclib; ABEMA-R, abemaciclib-resistant; ABEMA-S, abemaciclib-sensitive; ANZ, anastrozole; FDR, false discovery rate; NES, normalized enrichment score; PALBO, palbociclib; PALBO-R, palbociclib-resistant; PALBO-S, palbociclib-sensitive; pts, patients.

Author Manuscript

Author Manuscript

Author Manuscript

Author Manuscript

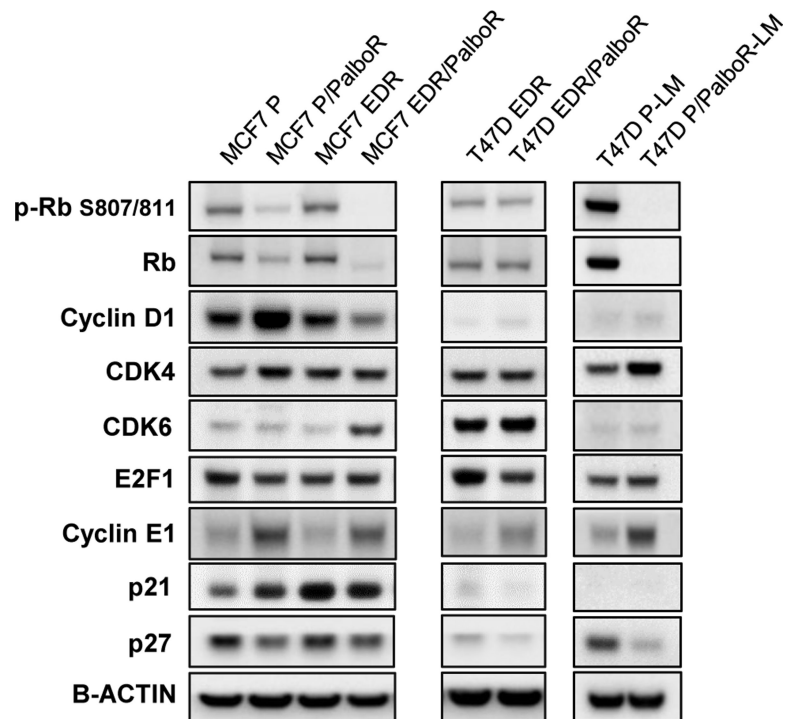


Figure 3. The cyclin D–CDK4/6–Rb axis is altered in ER+ cell lines with acquired resistance to palbociclib.

Protein (by Western blot) levels of selected G1/S cell cycle check point components in MCF7 P, MCF7 EDR, T47D P-LM, and T47D EDR cell lines and their palbociclib-resistant derivatives (PalboR). PalboR cell lines were cultured in the presence of 1 μ M palbociclib.

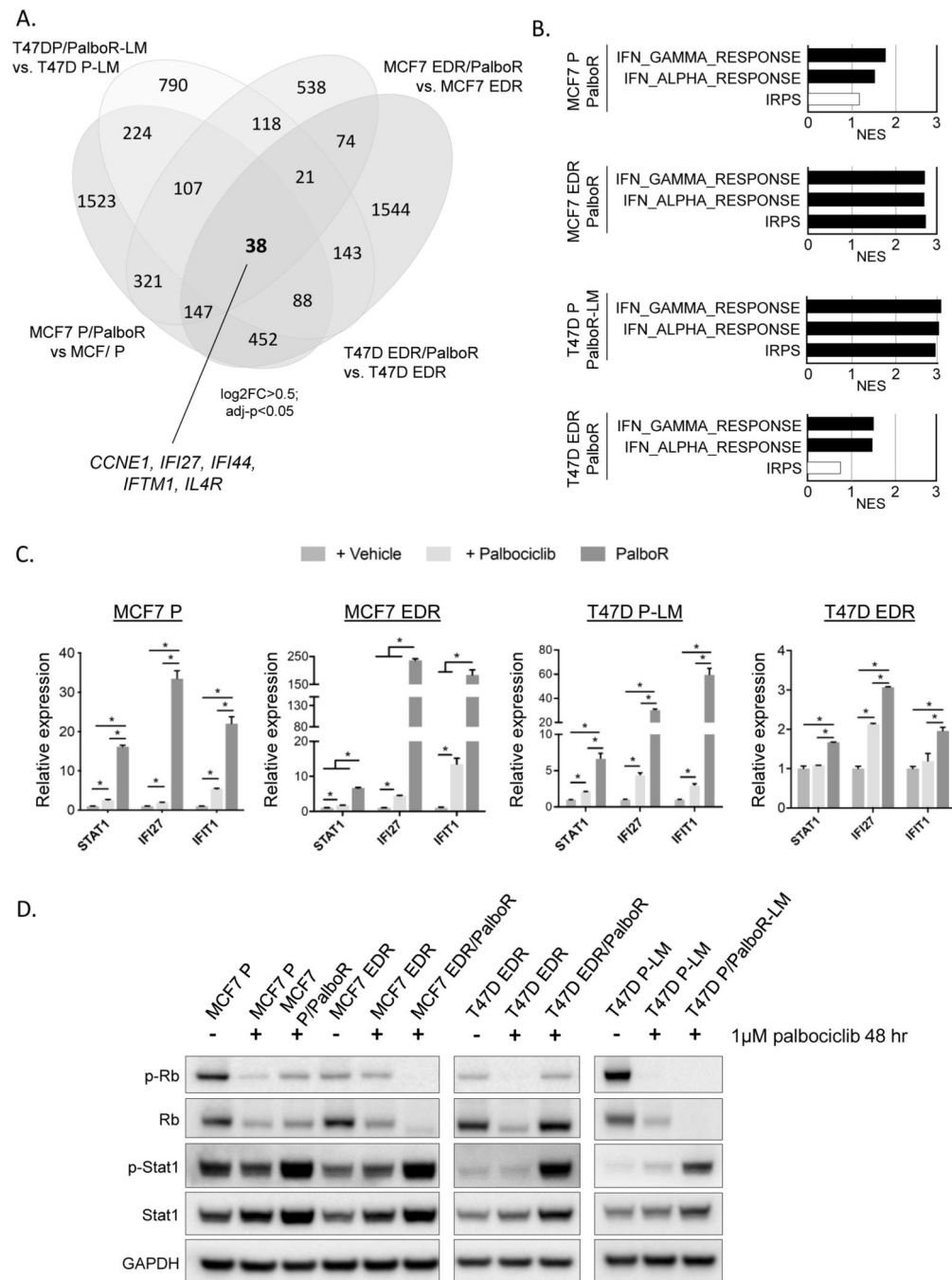


Figure 4. IFN-signaling is up-regulated in cells with acquired resistance to palbociclib.

A, Venn diagram representing overlap between significantly up-regulated genes [\log_2 fold-change (FC) > 0.5, $FDR < 0.05$] in MCF7 P/PalboR, MCF7 EDR/PalboR, T47D P/PalboR-LM, and T47D EDR/PalboR cell lines compared to their native counterparts. PalboR derivatives were grown in the presence 1 μ M palbociclib while MCF7 and T47D P-LM and EDR lines were maintained in their original media without palbociclib supplementation.

B, Bar plots showing IFN-alpha response, IFN-gamma response, and IRPS signature enrichments in MCF7 P, MCF7 EDR, T47D P-LM, and T47D EDR PalboR cell lines. Black

color indicates *FDR* value <0.05. **C**, qRT/PCR of selected IFN-stimulated genes (*STAT1*, *IFI27*, *IFIT1*) in MCF7 P, MCF7 EDR, T47D P-LM, and T47D EDR (± 48 hours 1 μ M palbociclib) and their PalboR derivatives. **D**, Western blot of p-Rb, Rb, p-Stat1, and Stat1 in MCF7 P, MCF7 EDR, T47D P-LM, and T47D EDR (± 48 hours 1 μ M palbociclib) and their PalboR derivatives. PalboR cell lines were cultured in the presence of 1 μ M palbociclib. * $P < 0.05$

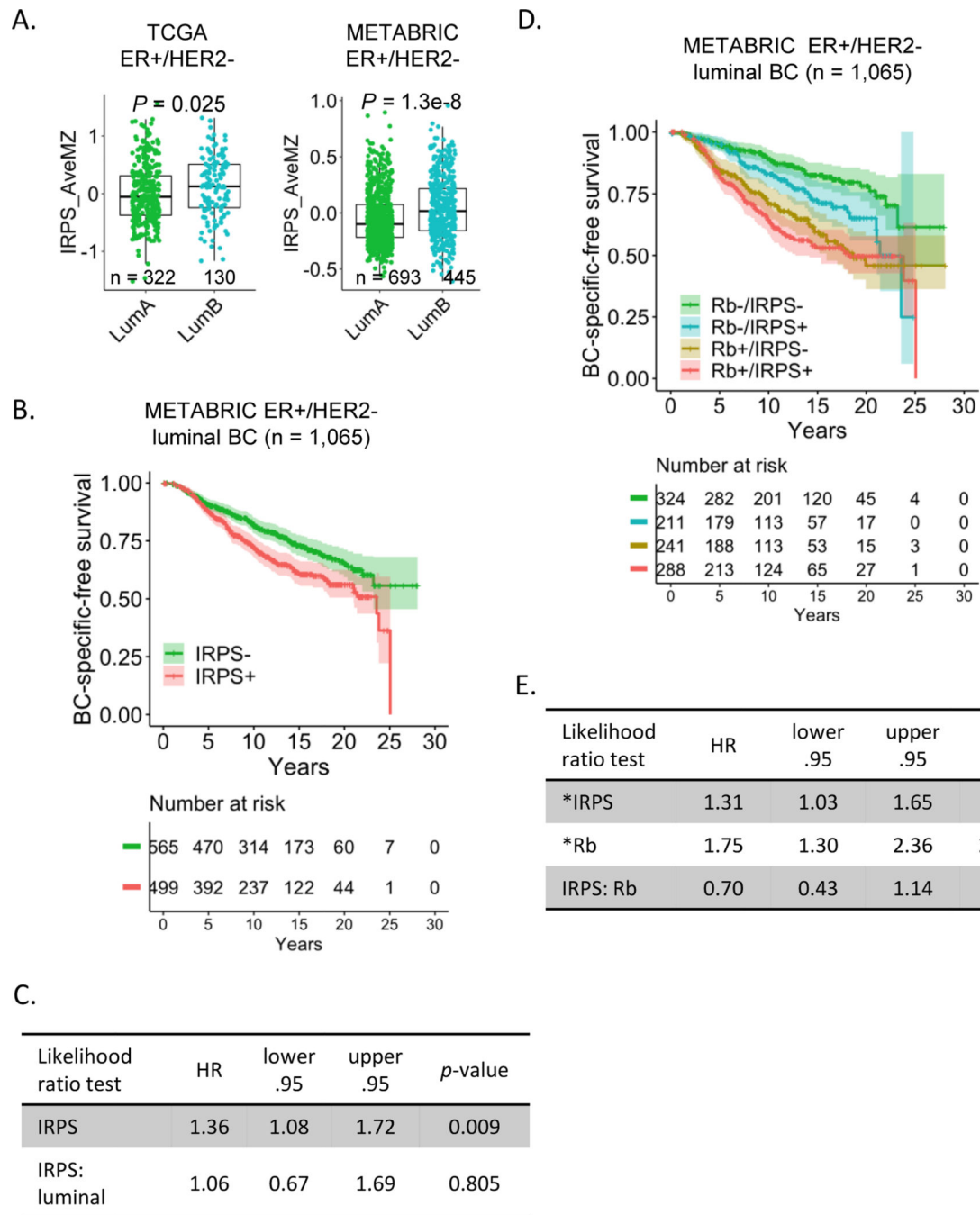


Figure 5. IRPS predicts poor prognosis in luminal BC patients.

A, Boxplots of IRPS scores, measured by average of modified z-score (AveMZ) of signature genes, in luminal A (LumA) vs. luminal B (LumB) subtype of ER+/HER2- tumors in TCGA ($n = 452$) and METABRIC ($n = 1,138$) datasets. **B**, Kaplan-Meier survival curves of BC-specific-free survival (BCSS) of patients with ER+/HER2- luminal tumors in the METABRIC dataset ($n = 1,065$, median follow-up time: 10 yrs) stratified by the median cut-off (-/+ denotes < and > median, respectively) of IRPS score. **C**, Type 2 likelihood ratio (LR) tests in the Cox proportional hazards model were used to calculate P values for

IRPS score in predicting outcome and the interaction between IRPS score and the luminal subtype. Luminal subtype was included in the model as a potential confounding factor because luminal subtype is associated with outcome and with differential IRPS values and RB status. **D**, Kaplan-Meier survival curves of BCSS of patients with ER+/HER2- luminal tumors in the METABRIC dataset ($n = 1,065$, median follow-up time: 10 yrs) stratified by the combination of the $-/+$ of median levels of IRPS and Rb scores. **E**, Type 2 likelihood ratio test in the Cox proportional hazards model using IRPS and Rb $-/+$ status and the luminal subtype as confounding factors. * Denotes the P value and HR of IRPS and Rb calculated from the main effects model after removing non-significant interactions. HR of interaction was derived using the full model including the interaction of IRPS and Rb status.

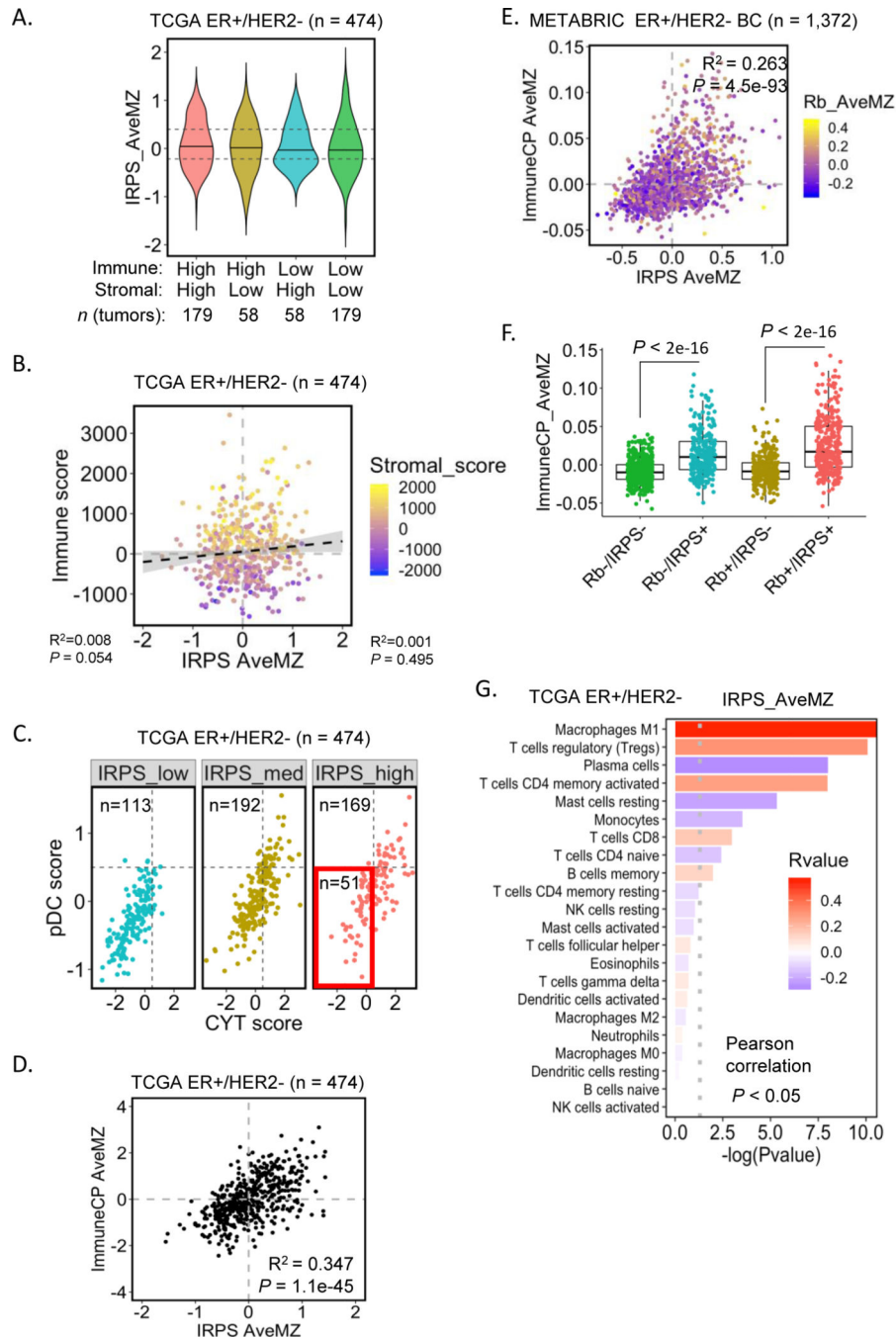


Figure 6. IRPS is associated with expression of immune checkpoints and an immunosuppressive tumor microenvironment in ER+/HER2- BC.

A, Association of IRPS score with immune or stromal infiltrations in ER+/HER2- breast tumors from the TCGA dataset (n = 474). The violin plots show the kernel probability density of the IRPS score with the median score in each subgroup as indicated by the black bars. Broken lines indicate score cutoffs for IRPS-high, -medium, and -low tumors. Four subgroups are divided based on the median of immune and stromal scores. Stromal and immune scores for each tumor were extracted from the ESTIMATE R-library. **B**, Scatter

plots of IRPS and immune scores of the same set of ER+/HER2- TCGA tumors. The color bar for each point indicates the range of stromal score. **C**, Scatter plots of CYT (perforin (PRF1) and granzyme A (GZMA) expression) and pDC scores in TCGA ER+/HER2- breast tumors ($n = 474$) classified into IRPS-low, -medium, and -high groups. The red box indicates tumors ($n = 51$) with IRPS-high but low CYT and pDC scores. **D**, Scatter plots of IRPS and immune checkpoint (CP) (PD-1, PD-L1, CTLA4) scores in TCGA ER+/HER2- breast tumors ($n = 474$). **E**, Scatter plots of IRPS and ImmuneCP scores in METABRIC ER+/HER2- tumors ($n = 1,372$). The color bar for each point indicates the range of the Rb score. All the scatter plots were analyzed by the Pearson's coefficient test. **F**, Boxplots showing the ImmuneCP scores across the four groups of METABRIC ER+/HER2- tumors ($n = 1,372$) stratified by the IRPS and Rb status with $-/+$ denoting \leq and $>$ median cut-off. P value was calculated by the pairwise t-test with the Bonferroni-adjusted method. **G**, Bar charts showing Pearson correlation between IRPS score and scores of immune components estimated by CIBERSORT in TCGA ER+/HER2- breast tumors ($n = 474$). The dotted line marks the significance of P value of 0.05. The color bar indicates the range of correlation coefficient R value.